



Published in final edited form as:

J Med Chem. 2006 July 27; 49(15): 4487–4496.

Novel sst₂-selective somatostatin agonists. Three-dimensional consensus structure by NMR

Christy Rani R. Grace¹, Judit Erchegyi², Steven C. Koerber², Jean Claude Reubi³, Jean Rivier^{2,*}, and Roland Riek¹

¹Structural Biology Laboratory, The Salk Institute for Biological Studies, 10010 N. Torrey Pines Road, La Jolla, CA 92037, USA ²The Clayton Foundation Laboratories for Peptide Biology, The Salk Institute for Biological Studies, 10010 N. Torrey Pines Road, La Jolla, CA 92037, USA ³Division of Cell Biology and Experimental Cancer Research, Institute of Pathology, University of Berne, Berne, Switzerland.

Abstract

The three-dimensional NMR structures of six octapeptide agonist analogues of somatostatin (SRIF) in the free form are described. These analogues, with the basic sequence H-DPhe/Phe²-c[Cys³-Xxx⁷-DTrp⁸-Lys⁹-Thr¹⁰-Cys¹⁴]-Thr-NH₂ (the numbering refers to the position in native SRIF), with Xxx⁷ being Ala/Aph, exhibit potent and highly selective binding to human SRIF type 2 (sst₂) receptors. The backbone of these sst₂-selective analogues have the usual type-II' β-turn reported in the literature for sst_{2/3/5}-subtype-selective analogues. Correlating biological results and NMR studies led to the identification of the side chains of DPhe², DTrp⁸ and Lys⁹ as the necessary components of the sst₂ pharmacophore. This is the first study to show that the aromatic ring at position 7 (Phe⁷) is not critical for sst₂ binding and that it plays an important role in sst₃ and sst₅ binding. This pharmacophore is therefore different from that proposed by others for sst_{2/3/5} analogues.

Introduction

Somatostatin (SRIF, H-Ala¹-Gly²-c[Cys³-Lys⁴-Asn⁵-Phe⁶-Phe⁷-Trp⁸-Lys⁹-Thr¹⁰-Phe¹¹-Thr¹²-Ser¹³-Cys¹⁴]-OH), a cyclic tetradecapeptide, isolated from the hypothalamus as a growth hormone inhibitor, is now known to be a multifunctional peptide located in most of the brain regions and in peripheral organs.^{1,2} Cells containing SRIF are typically neurons or endocrine-like cells which are found in high density throughout the central and peripheral nervous systems, in the endocrine pancreas, and in the gut and in small numbers in the thyroid, adrenals, submandibular glands, kidneys, prostate and placenta.^{1,2} The activities of SRIF are mediated through a family of five different high affinity membrane receptors, sst₁-sst₅ (sst_s). Due to its broad spectrum of physiological activities and its short duration of action due to rapid proteolytic degradation *in vivo*,³ SRIF continues to be a target for the development of subtype-specific analogues.⁴⁻⁷ (and references therein)

Indeed, over the last three decades, hundreds of SRIF analogues have been reported and tested in different biological systems including affinity and selectivity towards the five receptor-subtypes.⁸⁻¹⁰ Correspondingly, early structure-activity relationship (SAR) studies ruled out

*Corresponding author: Jean Rivier The Salk Institute The Clayton Foundation Laboratories for Peptide Biology 10010 N. Torrey Pines Road La Jolla, CA 92037 (858) 453-4100 Fax: (858) 552-1546 email: jrivier@salk.edu.

Abbreviations: The abbreviations for the common amino acids are in accordance with the recommendations of the IUPAC-IUB Joint Commission on Biochemical Nomenclature (Eur. J. Biochem. 1984, 138:9-37). The symbols represent the L-isomer except when indicated otherwise.

the specific involvement of the side chains of all residues but Phe⁷-DTrp⁸-Lys⁹ for biological recognition.¹¹⁻¹³ (**Note:** the numbering of residues follows that of native SRIF.) Extensive structural studies including NMR and x-ray diffraction¹⁴ were carried out to elucidate the pharmacophore and the consensus structural motif of analogues binding predominantly to sst_{2/5} (and sst₃) receptors. On the basis of these 3D structures of the free peptides, a pharmacophore model was proposed for SRIF analogues binding to sst_{2/5} (and sst₃).¹⁵⁻¹⁸ In this model, the side chains and the relative spatial arrangement of DPhe², Phe⁷, DTrp⁸ and Lys⁹ constitute the most essential elements necessary for binding (Figure 3C). The side chain of DTrp⁸ is in close proximity to the side chain of Lys⁹ (~5 Å), whereas the side chain of Phe⁷ is about 7–9 Å away from the side chain of DTrp⁸ and 9–11 Å from the side chain of Lys⁹. The aromatic side chain at position 2 outside the disulfide bond was not conserved in its position in most of these analogues. The distance between DPhe² and DTrp⁸, Lys⁹, Phe⁷ were 11–15 Å, 12–15 Å, 5–11 Å respectively.¹⁹ In this model of the pharmacophore, the rotamer of the side chains of DTrp⁸ and Phe⁷ are in the *trans* configuration and that of Lys⁹ is in the *gauche* configuration.

Recently, we have proposed models of the sst₄ and the sst₁ pharmacophores derived from the NMR consensus structures of several receptor selective analogues.^{20,21} These models of the pharmacophores are different from that of the reported sst_{2/3/5} selective pharmacophore in the following manner. The sst₄ pharmacophore has one aromatic side chain, either Phe⁶ or Phe¹¹ involved in binding in addition to the DTrp⁸ and Lys⁹ pair. The distance between DTrp⁸ and Lys⁹ is 4.5–6.5 Å, between DTrp⁸ and Phe^{6/11} is 5.5–9.5 Å and between Lys⁹ and Phe^{6/11} is 4.5–6.5 Å. The aromatic side chain of Phe^{6/11} is closer to the side chain of Lys⁹ than that of DTrp⁸ (Figure 3E). On the other hand, the sst₁ pharmacophore has two aromatic side chains, at position 6 or 7 and 11, involved in binding in addition to the DTrp⁸ and IAm⁹ pair. The positioning of the two aromatic side chains at the back of the peptide plane has to be noted, which is opposite to that of the sst₄ and sst_{2/3/5} pharmacophores. The sst₁ receptor selectivity is mainly achieved by the amino acid IAm, which replaces Lys at position 9. The distance between DTrp⁸ and IAm⁹ is 7–8 Å, between DTrp⁸ and Phe^{6/7} is 6–7.5 Å and between IAm⁹ and Phe¹¹ is 8–10 Å (Figure 3D).

In a similar manner, we present a model of the sst₂ pharmacophore based on the 3D NMR structures of the free peptides. The three-dimensional structures of six analogues in DMSO-d₆ are presented including the structure of octreotide amide. These analogues have the typical octreotide scaffold with a type-II' β-turn backbone conformation similar to that of the reported sst_{2/3/5} selective analogues, yet their pharmacophore has one aromatic side chain (Phe⁷) less than that of the reported sst_{2/3/5} selective analogues.

Results

Peptide synthesis and characterization are described in Table 1 and experimental section. The proton resonance assignment and the structure determination by NMR for each of the sst₂-selective analogues **1**–**6** (Table 1) are presented in Tables 2 and 3.

Assignment of proton resonances, collection of structural restraints, and structure determination

The nearly complete chemical shift assignment of proton resonances (Table 2) for analogues **1**–**6** (Table 1) has been carried out using two-dimensional (2D) NMR experiments applying the standard procedure described in the Experimental Section. The N-terminal amino protons for analogues **5** and **6** were not observed due to fast exchange with the solvent. The amide proton of DPhe²/Phe for analogues **2** and **3** were observed at high field due to the carbamylation of the N-terminus. Chemical shifts can provide insight into the structure of the peptides, which is particularly true for SRIF analogues. The ring current of the indole ring leads

to a distinct shift of the C γ protons of the sequential Lys side chain to lower frequencies when these groups are closer in space, as in a β -turn. The downfield shift of C γ protons has been observed in all of these sst₂-selective analogues, which is similar to the observations found in the non-selective analogues binding to sst_{2/3/5}.^{17,22-30} This indicates the presence of a β -turn around these residues in these analogues.

A large number of experimental NOEs is observed for all of the six analogues in the NOESY spectrum measured with a mixing time of 100 ms, leading to over 100 to 120 meaningful distance restraints per analogue and concomitantly \sim 15 restraints per residue, which is a typical number for folded proteins (Table 3). These structural restraints are used as input for the structure calculation with the program CYANA³¹ followed by restrained energy minimization using the program DISCOVER.³² The resulting bundle of 20 conformers per analogue represents the 3D structure of each analogue in solution. For each analogue, the small residual constraint violations in the distances for the 20 refined conformers (Table 3) and the coincidence of the experimental NOEs and short interatomic distances (data not shown) indicate that the input data represent a self-consistent set, and that the restraints are well satisfied in the calculated conformers (Table 3). The deviations from ideal geometry are minimal, and similar energy values are obtained for all of the 20 conformers for each analogue. The quality of the structures determined is reflected by the small backbone RMSD values relative to the mean coordinates of \sim 0.5 Å (see Table 3 and Figure 2).

Three-dimensional structure of H-DPhe²-c[Cys³-Ala⁷-DTrp⁸-Lys⁹-Thr¹⁰-Cys¹⁴]-Thr-NH₂(1)

Analogue **1** binds to receptor 2 with high affinity (IC₅₀ < 10 nM) and has an Ala at position 7. The quality of the structure is reflected by the small RMSD (Table 3), which can also be visually depicted from Figure 2 showing the bundle of 20 conformers representing the 3D structure. From the backbone torsion angles (Table 4), it can be seen that the backbone contains a β -turn of type-II' around DTrp⁸-Lys⁹. The β -turn is supported by the strong sequential $d_{\alpha\text{N}}(i,i+1)$ NOEs and medium-range $d_{\alpha\text{N}}(i,i+2)$ NOE (Figure 1) between DTrp⁸ and Thr¹⁰, as well as the hydrogen bond between Thr¹⁰NH-O'Ala⁷ in all the 20 structures. The low temperature coefficient observed for the amide proton of Thr¹⁰ (-1.1 ppb/K) confirms the presence of the hydrogen bond.³³ From the torsion angles listed in Table 4, it can be seen that the side chain of DTrp⁸ is in the *trans* rotamer, Lys⁹ is in the *gauche*⁺ rotamer and that of DPhe² is in the *gauche*⁻ rotamer.

Three-dimensional structure of H₂N-CO-DPhe²-c[Cys³-Aph(CONH₂)⁷-DTrp⁸-Lys⁹-Thr¹⁰-Cys¹⁴]-Thr-NH₂ (2)

Analogue **2** differs from analogue **1** at position 7 by the Aph(CONH₂) group as well as the N-terminal carbamoylation (Table 1). The backbone torsion angles (Table 4) indicate a β -turn of type-II' conformation around DTrp⁸-Lys⁹, which is supported by the medium range $d_{\alpha\text{N}}(i,i+2)$ NOE between DTrp⁸-Thr¹⁰ (Figure 1). The turn structure is further stabilized by the observed hydrogen bond between Thr¹⁰NH-O'Aph⁷ in most of the structures. The presence of the hydrogen bond is further confirmed by the unshifted amide proton resonance of Thr¹⁰ when the temperature was raised from 298K to 313K. The long range medium NOE observed between DPhe²(NH) and Thr¹⁰(HN) as well as the strong αH NOE observed between the cysteines stabilize the structure. The side chain of DPhe² is in the *gauche*⁺ rotamer, Aph⁷ and DTrp⁸ are in the *trans* rotamer and that of Lys⁹ is in the *gauche*⁻ rotamer (Table 4).

Three-dimensional structure of H₂N-CO-Phe²-c[Cys³-Aph(CONH₂)⁷-DTrp⁸-Lys⁹-Thr¹⁰-Cys¹⁴]-Thr-NH₂(3)

Analogue **3** binds selectively with high affinity to the sst₂ receptor and is different from analogue **2**, with a Phe at position 2. From the backbone torsion angles (Table 4), it can be seen that the backbone contains a β -turn of type-II' around DTrp⁸-Lys⁹. The β -turn is supported by

the medium-range $d_{\alpha\text{N}}(i,i+2)$ NOE and the weak $d_{\text{NN}}(i,i+2)$ NOE (Figure 1) between DTrp⁸ and Thr¹⁰, as well as the hydrogen bond Thr¹⁰NH-O'Aph⁷ observed in most of the 20 structures. The low temperature coefficient observed for the amide proton of Thr¹⁰ (-0.4 ppb/K) confirms the presence of the hydrogen bond.³³ In addition long range medium NOEs are observed between the amide protons of Phe² and Thr¹⁰ and the cysteins, which stabilizes the structure. The side chains of Phe², Aph⁷ and Lys⁹ are in the *gauche*⁺ rotamer and that of DTrp⁸ is in the *trans* rotamer (Table 4).

Three-dimensional structure of H₂N-CO-DPhe²-c[Cys³-Aph(CONHOCH₃)⁷-DTrp⁸-Lys⁹-Thr¹⁰-Cys¹⁴]-Thr-NH₂(4)

Analogue **4** binds selectively with nanomolar affinity to the sst₂ receptor. It differs from analogues **2** and **3** by the longer chain of Aph(CONHOCH₃) at position 7, which inhibits the binding to receptors 3 and 5 completely (Table 1). The backbone torsion angles indicate a β -turn of type-II' conformation around DTrp⁸-Lys⁹ (Table 4), which is supported by the medium-range $d_{\alpha\text{N}}(i,i+2)$ NOE and the weak $d_{\text{NN}}(i,i+2)$ NOE observed between DTrp⁸ and Thr¹⁰ (Figure 1). The unshifted amide proton resonance of Thr¹⁰ at 7.63 ppm (from 298K to 313K) suggests the presence of a hydrogen bond involving this amide proton, which has been observed in all the 20 structures. The side chain of DPhe² is in the *gauche*⁺ rotamer, Aph⁷ and DTrp⁸ are in the *trans* rotamer and that of Lys⁹ is in the *gauche*⁻ rotamer (Table 4). The other long range NOEs, which stabilize the structure, are observed between the amide proton of DPhe² and α H proton of Cys¹⁴ and the α H protons of the cysteins.

Three-dimensional structure of H-c[Cys³-Phe⁷-DTrp⁸-Lys⁹-Thr¹⁰-Cys¹⁴]-OH (5)

Analogue **5** is the shortest analogue, a cyclic hexapeptide containing only the core residues. Analogue **5** was synthesized to identify the role of _DPhe² in sst₂ binding. Indeed, it did not bind to all the five receptors (Table 1). From the backbone torsion angles it can be seen that it has a type-II' β -turn around DTrp⁸ and Lys⁹ (Table 4) and the turn is supported by the presence of the medium range $d_{\alpha\text{N}}(i,i+2)$ NOE observed between DTrp⁸ and Thr¹⁰ (Figure 1) as well as the hydrogen bond observed between Thr¹⁰NH-O'Phe⁷ in all of the 20 structures. The low temperature coefficient observed for the amide proton of Thr¹⁰ (-1.4 ppb/K) confirms the presence of the hydrogen bond.³³ The side chain of Phe⁷ and DTrp⁸ are in the *trans* rotamer and that of Lys⁹ is in the *gauche*⁺ rotamer (Table 4).

Three-dimensional structure of H-DPhe²-c[Cys³-Phe⁷-DTrp⁸-Lys⁹-Thr¹⁰-Cys¹⁴]-Thr-NH₂ (6)

Analogue **6**, which is very similar to octreotide (Thr-ol is substituted by Thr-NH₂), binds to the sst_{2/3/5} receptors with moderately high affinity (Table 1). The 3D structure of this analogue was obtained in order to compare the structure of octreotide with the other analogues under identical conditions. Melacini et al. reported that the backbone of Sandostatin (octreotide) could be in a conformational equilibrium between β -turn and helical structures in solvents different from DMSO.^{19,28} From the torsion angles, we observe a type-II' β -turn conformation for the backbone, which is supported by the presence of the medium range $d_{\alpha\text{N}}(i,i+2)$ NOE observed between DTrp⁸ and Thr¹⁰ (Figure 1) as well as the hydrogen bond observed between Thr¹⁰NH-O'Phe⁷ in all of the 20 structures. The unshifted amide proton resonance of Thr¹⁰ at 7.58 ppm (from 298K to 313K) confirms that this amide proton is involved in a hydrogen bond. The side chain of Phe⁷ and DTrp⁸ are in the *trans* rotamer and that of Lys⁹ is in the *gauche*⁺ rotamer (Table 4).

Discussion

We have recently proposed models of the sst₁ and sst₄ pharmacophores based on the 3D NMR structures of several receptor selective analogues. The sst₁ and sst₄ receptors have maximum sequence similarity and hence were assumed to be part of one close family, different from the

family of $ss_{2/3/5}$ receptors. Yet, the proposed ss_1 and ss_4 pharmacophores are completely distinct from each other. For example, the position and the number of aromatic rings involved in binding are different for the two ligands, suggesting that these hydrophobic residues interact with different regions of the ss_1 and ss_4 receptors, respectively (Figure 3D and 3E). On the other hand, most of the previously published analogues binding with high affinity to ss_2 receptor were also binding to ss_5 receptors with nM affinity and sometimes to ss_3 receptors as well. Melacini et al., proposed a pharmacophore model for these analogues binding non-selectively to all of the three receptors (Figure 3C).¹⁹ Here, we have identified the crucial residues involved in selective ss_2 binding, revealing subtle differences in the pharmacophores between the only ss_2 -selective analogues and the less selective $ss_{2/3/5}$ -selective analogues. In the $ss_{2/3/5}$ -selective pharmacophore found in octreotide and homologues, we identified two aromatic side chains (at position 2 and 7) in addition to the DTrp⁸ and Lys⁹ residues. Removal of the aromatic amino acid at position 2 (analogue 5) resulted in loss of binding to all of the three receptors (compare with analogue 6). This clearly confirms that residue 2 is important for binding to $ss_{2/3/5}$ receptors (Table 1). On the other hand, replacement of Phe at position 7 by Ala (analogue 1) resulted in selective binding (nM) to receptor 2. Hence, it can be concluded that this aromatic ring is not crucial for ss_2 binding, and is crucial for ss_3 and ss_5 binding, as the binding to receptors 3 and 5 decreased (Table 1). Replacement of Phe at position 7 by an amino acid having a longer side chain, such as Aph has also decreased the binding to ss_3 and ss_5 receptors, retaining high binding affinity to ss_2 receptors.

Three-dimensional structures of the ss_2 -selective analogues and the pharmacophore model

Most of the bioactive analogues of SRIF reported so far have a β -turn type either of type II' or type VI for the backbone conformation.^{13,15,17,18,24,34-39} The structures of all of the presented four ss_2 -selective analogues have also a β -turn of type-II' (Figure 2, Table 4). In these analogues, the side chain of DTrp⁸ is in the *trans* conformer and the side chain of Lys⁹ is either in the *gauche*⁺ or *gauche*⁻ conformer, bringing the two side chains adjacent to each other in a close proximity. The side chain of Phe or DPhe at position 2 is either in the *gauche*⁺ or *gauche*⁻ conformer, far from the DTrp-Lys pair and their position is conserved in all of the four analogues studied here (Figure 3A). Hence, we propose a pharmacophore model for ss_2 -selective analogues involving the three side chains, namely, the indole (DTrp) at position 8, the amino-alkyl (Lys) at position 9 and an aromatic ring at position 2 (Figure 3B). In addition, the right spatial arrangement of the indole ring, the lysine side chain and the aromatic ring of a phenylalanine is also important for ss_2 -selective binding. The proposed distances between the C γ of residue 8 and C γ of Phe² is 12–13.5 Å; C γ of residue 8 and C γ of Lys⁹ is 4–5 Å and C γ of Phe² and C γ of Lys⁹ is 12.5–15 Å. Conservative replacements of these residues do not change the binding affinities and receptor selectivity evidently.

Comparison of the ss_2 -selective versus $ss_{2/3/5}$ -selective pharmacophore

With the consensus structural motif for the ss_2 -selective SRIF analogues (Figures 3A and B), comparison between the ss_2 and the pharmacophore for $ss_{2/3/5}$ -selective analogues (Figure 3C) is possible. Interestingly, Goodman and coworkers illustrated that in SRIF analogues, which bind selectively to $ss_{2/3/5}$, the side chains of DTrp⁸, Lys⁹, Phe⁷ and Phe² constitute the most essential elements necessary for binding.^{15,16} In their pharmacophore model, DTrp⁸ and Lys⁹ were at a close proximity of ~5 Å, which is similar to the ss_2 pharmacophore. The aromatic ring at position 7, Phe⁷ is farther away from DTrp⁸ (7 to 9 Å) and Lys⁹ (9 to 11 Å), and is not present in the ss_2 pharmacophore. Hence Phe⁷ is not crucial for ss_2 receptor binding. The position of DPhe² in the ss_2 pharmacophore is highly conserved whereas it varies in the $ss_{2/3/5}$ pharmacophore. This difference can easily be seen from the superposition of the ss_2 -selective analogue 1 and the $ss_{2/3/5}$ -selective octreotide (Figure 4).¹⁶ They differ mostly in the position of the phenylalanine at position 2. Based on our studies reported here and the observation of Melacini et al.,¹⁹ octreotide undergoes a conformational exchange between β -

turn and helical backbone conformation, it can be proposed that octreotide undergoes conformational change to fit into both the sst₂ and sst₅ pharmacophores. It should prefer the β -turn conformation, where the DPhe² is close to the sst₂ pharmacophore (Figure 4A) and must prefer the helical conformation to fit the sst₅ pharmacophore (Figure 4B), where DPhe² is further away from the sst₂ pharmacophore (this hypothesis is further supported by unpublished results of sst₅ selective analogues). This conformational flexibility is therefore necessary to explain the non-selective binding of the octreotide type of analogues to sst_{2/3/5} receptors simultaneously.

Comparison of the sst₂-selective versus sst₁- and sst₄-selective pharmacophores

Since three different pharmacophores are available for the subtype-selective analogues, namely, 1, 2 and 4, the differences among these subtype-selective pharmacophores can be discussed with respect to sst₂ pharmacophore (Figure 3B). The sst₁ pharmacophore has two aromatic side chains important for binding and they are closer to DTrp-IAMP pair and are present on the back side of the peptide, compared to the sst₂ pharmacophore, where one aromatic ring important for binding is far from DTrp-Lys pair. Also IAMP at position 9 crucial for sst₁ selectivity is further away from DTrp⁸, compared to the other pharmacophores, where Lys at position 9 is closer to DTrp⁸. The sst₄ pharmacophore is somewhat similar to sst₂ pharmacophore in the number of interacting residues with the receptors, namely DTrp⁸, Lys⁹ and one aromatic side chain either at position 6 or 11. But the position of the aromatic side chain is closer to the DTrp-Lys pair in the sst₄ pharmacophore, whereas it is farther away in the sst₂ pharmacophore. Hence, these subtype-selective pharmacophores explain why the sst₂-selective analogues did not bind to other receptors of SRIF, specifically to 1 and 4.

Conclusions

The 3D conformations of four cyclic SRIF octapeptide analogues with a hexapeptide core having high binding affinity and selectivity to the sst₂ receptor have been presented. These studies indicate that these analogues have a β -turn of type-II' for the backbone conformation which orients the side chains of the essentially important residues, namely indole at position 8, amino alkyl group at position 9 and an aromatic ring outside the cycle, in their respective positions for effective receptor-ligand binding. Based on this, we have proposed the SRIF binding motif for the sst₂ receptor consisting of these three side chains, namely DTrp⁸, Lys⁹ and DPhe². This binding motif differs from the binding motif for sst₂/sst₃/sst₅-selective receptors by one less aromatic side chain at position 7 (Figure 3). Furthermore, the model proposed also explains the selective binding of the non-peptoid analogues of SRIF agonists.⁴⁰⁻⁴³ The pharmacophore models proposed so far enable us to understand the binding of several other SRIF analogues to somatostatin receptors and will play an important role in designing highly selective peptides as well as non-peptide ligands of SRIF.

Experimental Section

Peptide synthesis, purification and characterization

Starting Materials—4-methylbenzhydramine resin (MBHA) with the capacity of 0.4 mmol/g and Boc-Cys(Mob)-CM resin with a capacity of 0.3–0.4 mmol/g were used. All Boc-N α -protected amino acids were commercially available (Chem Impex, Wood Dale, IL, Reanal Finechemical Co., Budapest, Hungary), except Boc-Aph(Fmoc) which was synthesized in our laboratory.⁴⁴

Synthesis and Purification—Peptides were synthesized by SPPS methodology following the Boc strategy and purified as we published earlier.⁴⁵ The -CO-NH₂ (Cbm) ureido group at the 4-amino function of Aph and at the N-terminus of the peptides was introduced

simultaneously on the resin. The 4-amino function of Aph was freed with 20% piperidine in NMP and the N-terminus Boc was deprotected with 50% TFA in DCM after completion of the synthesis, then the carbamoylation was carried out with NaOCN (200 mg, 1.3 mmol) in NMP (8 mL) and glacial acetic acid (6 mL) per gram of initial resin. The ureido group -CO-NHOCH₃ (Cbm-OMe) at the 4-amino function of Aph (analogue 4) was also introduced on the resin. The N α -Boc protected resin-bound hexapeptide Boc-Aph(Fmoc)-DTrp-Lys[Z(2Cl)]-Thr(Bzl)-Cys(Mob)-Thr(Bzl)-MBHA was treated with 20% piperidine in NMP to free the 4-amino function of Aph and CH₃O-NH-COOC₆H₄-NO₂ (10 fold excess) in the presence of DIPEA in NMP was added to the resin which was shaken at RT for 4 h as we described earlier.⁴⁶ After completion of the synthesis, N-terminus Boc was deprotected with 50% TFA in DCM and the carbamoylation was carried out as described above. The completed peptides were cleaved from the resin by HF containing the scavengers anisole (10% v/v) and methyl sulfide (5% v/v) for 60 min at 0 °C. The diethyl ether precipitated crude peptides were cyclized in 75% acetic acid (200 mL) by addition of iodine (10% solution in methanol) until the appearance of a stable orange color. Forty minutes later, ascorbic acid was added to quench the excess of iodine. The crude, lyophilized peptides were purified by preparative RP-HPLC.⁴⁷

Characterization—The purity of the final peptides was determined by analytical RP-HPLC, CZE analysis.⁴⁸ (See legend of Table 1 for details.) Each peptide showed a purity of >95% by these methods. The observed monoisotopic (M + H)⁺ values of each peptide corresponded with the calculated (M + H)⁺ values.

Sample preparation and NMR Experiments

Peptides were synthesized on solid-phase with Boc chemistry on a CS-Bio Peptide Synthesizer (Model CS536).⁴⁻⁶ Anhydrous HF cleaved the products from the resin support with simultaneous side chain deprotection. The diethyl ether precipitated crude peptides were cyclized in 75% acetic acid by the addition of iodine (10% solution in methanol). All peptides were purified by preparative RP-HPLC. The purity of the final products was determined by analytical RP-HPLC and CZE. They were >95% pure by both methods. The products were also characterized by mass spectroscopy; the observed (M+H)⁺ values coincided with the calculated (M+H)⁺ values.

NMR samples were prepared by dissolving 2 mg of the analogue in 0.5 mL of DMSO-d₆. The ¹H NMR spectra were recorded on a Bruker 700 MHz spectrometer operating at proton frequency of 700 MHz. Chemical shifts were measured using DMSO (δ = 2.49 ppm) as an internal standard. The 1D spectra were also acquired at temperatures between 298 and 318 K and were utilized to measure the temperature coefficients of the amide resonances. All the 2D spectra were acquired at 298 K. Resonance assignments of the various proton resonances have been carried out using total correlation spectroscopy (TOCSY);^{49,50} double-quantum filtered spectroscopy (DQF-COSY)⁵¹ and nuclear Overhauser enhancement spectroscopy (NOESY).⁵²⁻⁵⁴ The TOCSY experiments employed the MLEV-17 spin-locking sequence suggested by Davis and Bax,⁴⁹ applied for a mixing time of 50 ms. The NOESY experiments were carried out with a mixing time of 100 ms. The TOCSY and NOESY spectra were acquired using 800 complex data points in the ω_1 dimension and 1024 complex data points in the ω_2 dimension with $t_{1\max}$ = 47 ms and $t_{2\max}$ = 120 ms and were subsequently zero-filled to 1024 \times 2048 before Fourier transformation. The DQF-COSY spectra were acquired with 1024 \times 4096 data points and were zero-filled to 2048 \times 4096 before Fourier transformation. The TOCSY, DQF-COSY and NOESY spectra were acquired with 8, 8 and 16 scans, respectively, with a relaxation delay of 1 s. The signal from the residual water of the solvent was suppressed using pre-saturation during the relaxation delay and during the mixing time. The TOCSY and NOESY data were multiplied by 75° shifted sine-function in both dimensions. All the spectra were

processed using the software PROSA.⁵⁵ The spectra were analyzed using the software X-EASY.⁵⁶

Structure Determination

The chemical shift assignment of the major conformer (the population of the minor conformer was < 10%) was obtained by the standard procedure using DQF-COSY and TOCSY spectra for intra-residual assignment and the NOESY spectrum was used for the sequential assignment.⁵⁷ The collection of structural restraints was based on the NOEs and vicinal $^3J_{\text{NH}\alpha}$ couplings. Dihedral angle constraints were obtained from the $^3J_{\text{NH}\alpha}$ couplings, which were measured from the 1D ^1H NMR spectra and from the intra-residual and sequential NOEs along with the macro GRIDSEARCH in the program CYANA.³¹ The calibration of NOE intensities versus ^1H - ^1H distance restraints and appropriate pseudo-atom corrections to the non-stereo specifically assigned methylene, methyl and ring protons were performed using the program CYANA. On an average, approximately 100 NOE constraints and 20 angle constraints were utilized while calculating the conformers (Table 3). A total of 100 conformers were initially generated by CYANA and a bundle containing 20 CYANA conformers with the lowest target function values were utilized for further restrained energy minimization, using the CFF91 force field⁵⁸ with the energy criteria fit $0.1 \text{ kCal/mol/\AA}^59$ in the program DISCOVER with steepest decent and conjugate gradient algorithms.⁶⁰ The resulting energy minimized bundle of 20 conformers was used as a basis for discussing the solution conformation of the different SRIF analogues. The structures were analyzed using the program MOLMOL.⁶¹

Acknowledgments

This work was supported in part by NIH grants DK-50124 and DK-59953. We thank Drs. D. Hoyer, T. Reisine and S. Schulz for the gift of sst1-5 transfected CHO-K1, CCL39 or HEK293 cells. We thank Dr. W. Fisher and W. Low for mass spectrometric analyses, R. Kaiser, C. Miller, and B. Waser for technical assistance in the synthesis and characterization of some peptides and biological testing. We are indebted to D. Doan for manuscript preparation. J. R. is The Dr. Frederik Paulsen Chair in Neurosciences Professor. We thank the H. and J. Weinberg Foundation, the H. N. and F. C. Berger Foundation and the Auen Foundation for financial support. R. R. is the Pioneer Fund development Chair.

Additional abbreviations

Amp, 4-aminomethylphenylalanine
Aph, 4-amino-phenylalanine
CYANA, Combined assignment and dynamics algorithm for NMR applications
DMSO, dimethylsulfoxide
DQF-COSY, double quantum filtered correlation spectroscopy
IAmp, 4-(N-Isopropyl)-aminomethyl-phenylalanine
NMR, nuclear magnetic resonance
NOESY, nuclear Overhauser enhancement spectroscopy
3D, three-dimensional
PROSA, Processing algorithms
RMSD, root mean square deviation
SAR, structure activity relationships
SRIF, somatostatin
TOCSY, total correlation spectroscopy.

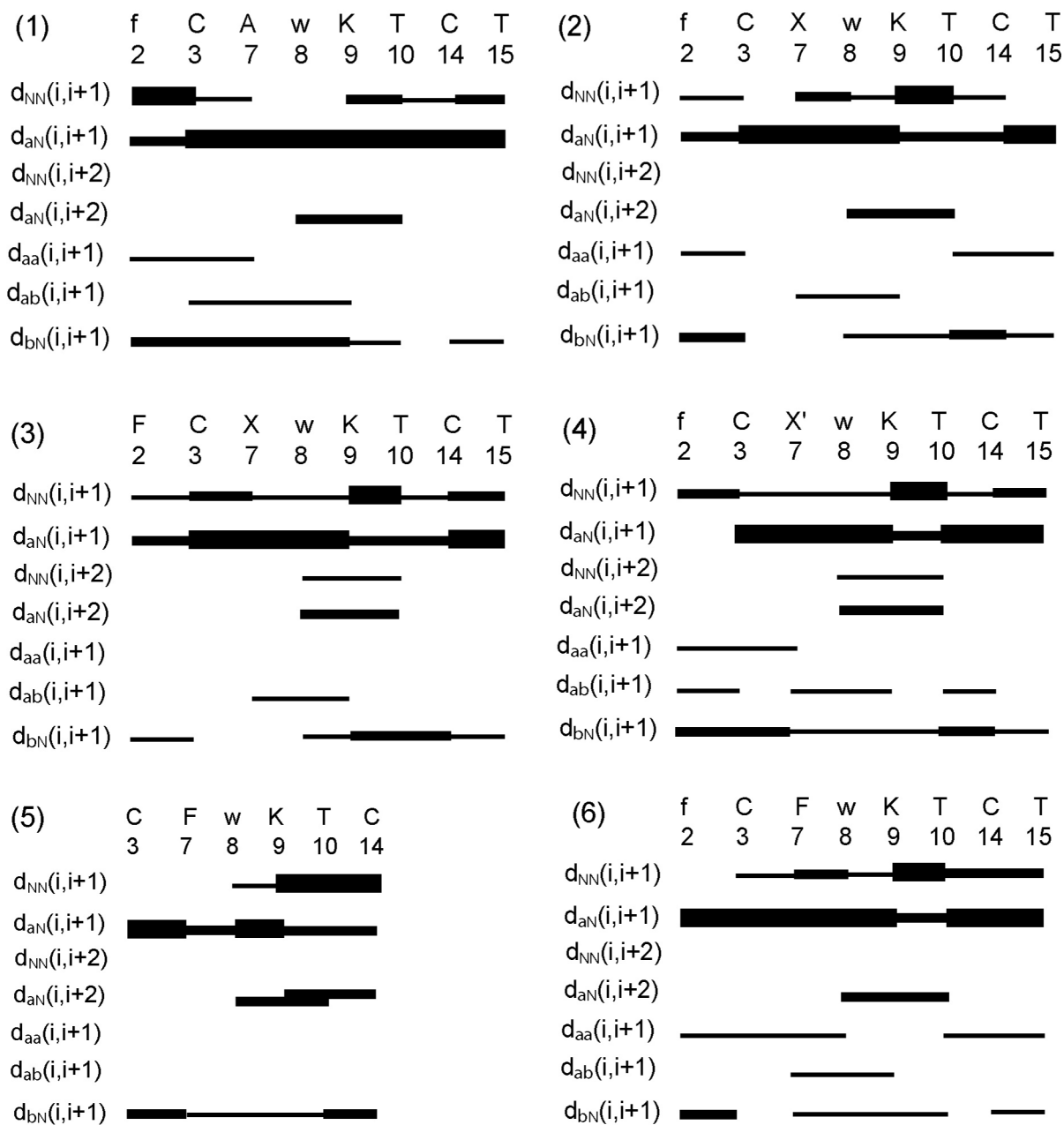
References

1. Reichlin S. Somatostatin. *N. Engl. J. Med* 1983;309:1495–1501. [PubMed: 6139753]
2. Reichlin S. Somatostatin (second of two parts). *N. Engl. J. Med* 1983;309:1556–1563. [PubMed: 6140639]

3. Patel YC, Wheatley T. In vivo and in vitro plasma disappearance and metabolism of somatostatin-28 and somatostatin-14 in the rat. *Endocrinology* 1983;112:220–225. [PubMed: 6128222]
4. Rivier J, Erchegyi J, Hoeger C, Miller C, Low W, Wenger S, Waser B, Schaer J-C, Reubi JC. Novel sst₄-selective somatostatin (SRIF) agonists. Part I: Lead identification using a betide scan. *J. Med. Chem* 2003;46:5579–5586. [PubMed: 14667212]
5. Erchegyi J, Penke B, Simon L, Michaelson S, Wenger S, Waser B, Cescato R, Schaer J-C, Reubi JC, Rivier J. Novel sst₄-selective somatostatin (SRIF) agonists. Part II: Analogues with β -methyl-3-(2-naphthyl)-alanine substitutions at position 8. *J. Med. Chem* 2003;46:5587–5596. [PubMed: 14667213]
6. Erchegyi J, Waser B, Schaer J-C, Cescato R, Brazeau JF, Rivier J, Reubi JC. Novel sst₄-selective somatostatin (SRIF) agonists. Part III: Analogues amenable to radiolabeling. *J. Med. Chem* 2003;46:5597–5605. [PubMed: 14667214]
7. Lewis I, Bauer W, Albert R, Chandramouli N, Pless J, Weckbecker G, Bruns C. A novel somatostatin mimic with broad somatotropin release inhibitory factor receptor binding and superior therapeutic potential. *J. Med. Chem* 2003;46:2334–2344. [PubMed: 12773038]
8. Moller LN, Stidsen CE, Hartmann B, Holst JJ. Somatostatin receptors. *Biochim. Biophys. Acta* 2003;1616:1–84. [PubMed: 14507421]
9. Olias G, Viollet C, Kusserow H, Epelbaum J, Meyerhof W. Regulation and function of somatostatin receptors. *J. Neurochem* 2004;89:1057–1091. [PubMed: 15147500]
10. Reubi JC, Waser B, Schaer J-C, Laissue JA. Somatostatin receptor sst1-sst5 expression in normal and neoplastic human tissues using receptor autoradiography with subtype-selective ligands. *Eur. J. Nucl. Med* 2001;28:836–846. [PubMed: 11504080]
11. Vale, W.; Rivier, C.; Brown, M.; Rivier, J. *Hypothalamic Peptide Hormones and Pituitary Regulation: Advances in Experimental Medicine and Biology*. Plenum Press; New York: 1977. Pharmacology of TRF, LRF and somatostatin.; p. 123-156.
12. Vale W, Rivier J, Ling N, Brown M. Biologic and immunologic activities and applications of somatostatin analogs. *Metabolism* 1978;27:1391–1401. [PubMed: 210361]
13. Veber DF, Freidinger RM, Perlow DS, Paleveda WJ Jr, Holly FW, Strachan RG, Nutt RF, Arison BH, Homnick C, Randall WC, Glitzer MS, Saperstein R, Hirschmann R. A potent cyclic hexapeptide analogue of somatostatin. *Nature (Lond)* 1981;292:55–58. [PubMed: 6116194]
14. Pohl E, Heine A, Sheldrick GM, Dauter Z, Wilson KS, Kallen J, Huber W, Pfaffli PJ. Structure of octreotide, a somatostatin analogue *Acta Crystallogr* 1995;51:48–59.
15. Huang Z, He Y, Raynor K, Tallent M, Reisine T, Goodman M. Side chain chiral methylated somatostatin analog synthesis and conformational analysis. *J. Am. Chem. Soc* 1992;114:9390–9401.
16. Melacini G, Zhu Q, Osapay G, Goodman M. A refined model for the somatostatin pharmacophore: Conformational analysis of lanthionine-sandostatin analogs. *J. Med. Chem* 1997;40:2252–2258. [PubMed: 9216844]
17. Mattern R-H, Tran T-A, Goodman M. Conformational analyses by ¹H NMR and computer simulations of cyclic hexapeptides related to somatostatin containing acidic and basic peptoid residues. *J. Pept. Res* 1999;53:146–160. [PubMed: 10195452]
18. Mattern RH, Tran TA, Goodman M. Conformational analyses of cyclic hexapeptide analogs of somatostatin containing arylalkyl peptoid and naphthylalanine residues. *J. Pept. Sci* 1999;5:161–175. [PubMed: 10323196]
19. Melacini G, Zhu Q, Goodman M. Multiconformational NMR analysis of sandostatin (octreotide): Equilibrium between β -sheet and partially helical structures. *Biochemistry* 1997;36:1233–1241. [PubMed: 9063871]
20. Grace CRR, Erchegyi J, Koerber SC, Reubi JC, Rivier J, Riek R. Novel sst₄-selective somatostatin (SRIF) agonists. Part IV: Three-dimensional consensus structure by NMR. *J. Med. Chem* 2003;46:5606–5618. [PubMed: 14667215]
21. Erchegyi, J.; Kirby, D.; Hoeger, C.; Koerber, SC.; Low, W.; Waser, B.; Eltschinger, V.; Schaer, J-C.; Cescato, R.; Grace, CRR.; Reubi, JC.; Riek, R.; Rivier, JE. Design of somatostatin (SRIF) receptor 1- and 4-selective ligands.. *Peptides 2004 - Proceedings of the 3rd International and 28th European Peptide Symposium*; Kenes International: Prague, Czech Republic. 2004. p. 180-181.

22. Wynants C, Van Binst G, Loosli HR. SMS 201–995, a very potent analogue of somatostatin. Assignment of the ^1H 500 MHz n.m.r. spectra and conformational analysis in aqueous solution. *Int. J. Pept. Prot. Res* 1985;25:608–614.
23. Kessler H, Haupt A, Schudok M, Ziegler K, Frimmer M. Peptide conformations. 49(1): synthesis and structure-activity relationships of side chain modified peptides of cyclo-(d-Pro-Phe-Thr-Lys-Trp-Phe-). *International Journal of Peptide and Protein Research* 1988;32:183–193. [PubMed: 2907513]
24. Mierke DF, Pattaroni C, Delaet N, Toy A, Goodman M, Tancredi T, Motta A, Temussi PA, Moroder L, Bovermann G, Wünsch E. Cyclic hexapeptides related to somatostatin. *Int. J. Pept. Prot. Res* 1990;36:418–432.
25. He Y-B, Huang Z, Raynor K, Reisine T, Goodman M. Syntheses and conformations of somatostatin-related cyclic hexapeptides incorporating specific alpha and beta-methylated residues. *J. Am. Chem. Soc* 1993;115:8066–8072.
26. Jaspers H, Horváth A, Mezö I, Kéri G, Van Binst G. Conformational study of a series of somatostatin analogues with antitumor and/or GH inhibitory activity. *Int. J. Pept. Prot. Res* 1994;43:271–276.
27. Gilon C, Huenges M, Mathä B, Gellerman G, Hornik V, Afargan M, Amitay O, Ziv O, Feller E, Gamliel A, Shohat D, Wanger M, Arad O, Kessler H. A backbone-cyclic, receptor 5-selective somatostatin analogue: Synthesis, bioactivity, and nuclear magnetic resonance conformational analysis. *J. Med. Chem* 1998;41:919–929. [PubMed: 9526566]
28. Mattern R-H, Zhang L, Rueter JK, Goodman M. Conformational analyses of sandostatin analogs containing stereochemical changes in positions 6 or 8. *Biopolymers* 2000;53:506–522. [PubMed: 10775066]
29. Cheng RP, Suich DJ, Cheng H, Roder H, DeGrado WF. Template-constrained somatostatin analogues: a biphenyl linker induces a type-V' turn. *J. Am. Chem. Soc* 2001;123:12710–12711. [PubMed: 11741449]
30. Jiang S, Gazal S, Gelerman G, Ziv O, Karpov O, Litman P, Bracha M, Afargan M, Gilon C, Goodman M. A bioactive somatostatin analog without a type II' beta-turn: synthesis and conformational analysis in solution. *J. Pept. Sci* 2001;7:521–528. [PubMed: 11695647]
31. Güntert P, Mumenthaler C, Wüthrich K. Torsion angle dynamics for NMR structure calculation with the new program DYANA. *J. Mol. Biol* 1997;273:283–298. [PubMed: 9367762]
32. Hagler AT, Dauber P, Osguthorpe DJ, Hempel JC. Dynamics and conformational energetics of a peptide hormone: vasopressin. *Science* 1985;227:1309–1315. [PubMed: 3975616]
33. Andersen NH, Neidigh JW, Harris SM, Lee GM, Liu Z, Tong H. Extracting information from the temperature gradients of polypeptide NH chemical shifts. 1. The importance of conformational averaging. *J. Am. Chem. Soc* 1997;119:8547–8561.
34. Arison BH, Hirschmann R, Veber DF. Inferences about the conformation of somatostatin at a biologic receptor based on NMR studies. *Bioorg. Chem* 1978;7
35. Kessler H, Griesinger C, Lautz J, Muller A, van Gunsteren WF, Berendsen HJC. Conformational dynamics detected by nuclear magnetic resonance NOE values and J coupling constants. *J. Am. Chem. Soc* 1988;110:3393–3396.
36. Huang A, Pröbstl A, Spencer JR, Yamazaki T, Goodman M. Cyclic hexapeptide analogs of somatostatin containing bridge modifications. *Int. J. Pept. Prot. Res* 1993;42:352–365.
37. Mattern R-H, Tran T-A, Goodman M. Conformational analyses of somatostatin-related cyclic hexapeptides containing peptoid residues. *J. Med. Chem* 1998;41:2686–2692. [PubMed: 9667959]
38. Falb E, Salitra Y, Yechezkel T, Bracha M, Litman P, Olender R, Rosenfeld R, Senderowitz H, Jiang S, Goodman M. A bicyclic and hsst2 selective somatostatin analogue: design, synthesis, conformational analysis and binding. *Bioorg. Med. Chem* 2001;9:3255–3264. [PubMed: 11711301]
39. Veber, DF. Design and discovery in the development of peptide analogs.. Twelfth American Peptide Symposium; Peptides: Chemistry and Biology: Cambridge, Mass. June 16–21, 1991; 1991. p. 1-14.
40. Ankersen M, Crider M, Liu S, Ho B, Andersen HS, Stidsen C. Discovery of a novel non-peptide somatostatin agonist with SST4 selectivity. *J. Am. Chem. Soc* 1998;120:1368–1373.
41. Liu S, Tang C, Ho B, Ankersen M, Stidsen CE, Crider AM. Nonpeptide somatostatin agonists with sst4 selectivity: Synthesis and structure-activity relationships of thioureas. *J. Med. Chem* 1998;41:4693–4705. [PubMed: 9822540]

42. Rohrer SP, Birzin ET, Mosley RT, Berk SC, Hutchins SM, Shen D-M, Xiong Y, Hayes EC, Parmar RM, Foor F, Mitra SW, Degrado SJ, Shu M, Klopp JM, Cai S-J, Blake A, Chan WWS, Pasternak A, Yang L, Patchett AA, Smith RG, Chapman KT, Schaeffer JM. Rapid identification of subtype-selective agonists of the somatostatin receptor through combinatorial chemistry. *Science* 1998;282:737–740. [PubMed: 9784130]
43. Prasad V, Birzin ET, McVaugh CT, Van Rijn RD, Rohrer SP, Chicchi G, Underwood DJ, Thornton ER, Smith AB 3rd, Hirschmann R. Effects of heterocyclic aromatic substituents on binding affinities at two distinct sites of somatostatin receptors. Correlation with the electrostatic potential of the substituents. *J. Med. Chem* 2003;46:1858–1869. [PubMed: 12723949]
44. Theobald P, Porter J, Rivier C, Corrigan A, Perrin M, Vale W, Rivier J. Novel gonadotropin releasing hormone antagonist: Peptides incorporating modified N⁰-cyanoguanidino moieties. *J. Med. Chem* 1991;34:2395–2402. [PubMed: 1714956]
45. Reubi JC, Schaer J-C, Wenger S, Hoeger C, Erchegyi J, Waser B, Rivier J. SST3-selective potent peptidic somatostatin receptor antagonists. *Proc. Natl. Acad. Sci. USA* 2000;97:13973–13978. [PubMed: 11095748]
46. Samant, MP.; Grace, CRR.; Hong, DJ.; Croston, G.; Riek, R.; Rivier, C.; Rivier, J. Novel analogues of degarelix incorporating hydroxy-, methoxy- and pegylated- urea moieties at residues 3, 5, 6 and the N-terminus. Part III. 2006.
47. Miller C, Rivier J. Peptide chemistry: Development of high-performance liquid chromatography and capillary zone electrophoresis. *Biopolymers Pept. Sci* 1996;40:265–317.
48. Miller C, Rivier J. Analysis of synthetic peptides by capillary zone electrophoresis in organic/aqueous buffers. *J. Pept. Res* 1998;51:444–451. [PubMed: 9650719]
49. Davis DG, Bax A. Assignment of complex ¹H NMR spectra via two-dimensional homonuclear Hartmann-Hahn spectroscopy. *J. Am. Chem. Soc* 1985;107:2820–2821.
50. Braunschweiler L, Ernst RR. Coherence transfer by isotropic mixing: Application to proton correlation spectroscopy. *J. Magn. Reson* 1983;53:521–528.
51. Rance M, Sorensen OW, Bodenhausen B, Wagner G, Ernst RR, Wüthrich K. Improved spectral resolution in COSY 1H NMR spectra of proteins via double quantum filtering. *Biochem. Biophys. Res. Commun* 1983;117:479–485. [PubMed: 6661238]
52. Kumar A, Wagner G, Ernst RR, Wüthrich K. Buildup rates of the nuclear Overhauser effect measured by two-dimensional proton magnetic resonance spectroscopy: Implications for studies of protein conformation. *J. Am. Chem. Soc* 1981;103:3654–3658.
53. Macura S, Ernst RR. Elucidation of cross-relaxation in liquids by two-dimensional NMR spectroscopy. *Mol. Phys* 1980;41:95–117.
54. Macura S, Huang Y, Suter D, Ernst RR. Two-dimensional chemical exchange and cross-relaxation spectroscopy of coupled nuclear spins. *J. Magn. Reson* 1981;43:259–281.
55. Güntert P, Dotsch V, Wider G, Wüthrich K. Processing of multi-dimensional NMR data with the new software PROSA. *J. Biomol. NMR* 1992;2:619–629.
56. Eccles C, Güntert P, Billeter M, Wüthrich K. Efficient analysis of protein 2D NMR spectra using the software package EASY. *J. Biomol. NMR* 1991;1:111–130. [PubMed: 1726780]
57. Wüthrich, K. *NMR of Proteins and Nucleic Acids*. J. Wiley & Sons; New York: 1986.
58. Maple JR, Thacher TS, Dinur U, Hagler AT. Biosym force field research results in new techniques for the extraction of inter- and intramolecular forces. *Chem. Design Auto. News* 1990;5:5–10.
59. Koerber SC, Rizo J, Struthers RS, Rivier JE. Consensus bioactive conformation of cyclic GnRH antagonists defined by NMR and molecular modeling. *J. Med. Chem* 2000;43:819–828. [PubMed: 10715150]
60. Hagler, AT. *The Peptides: Analysis, Synthesis, Biology*. Academic Press; Orlando, FL: 1985. Theoretical simulation of conformation, energetics and dynamics of peptides.; p. 213-299.
61. Koradi R, Billeter M. MOLMOL: a program for display and analysis of macromolecular structures. *PDB Newsletter* 1998;84:5–7.
62. Grace CRR, Durrer L, Koerber SC, Erchegyi J, Reubi JC, Rivier JE, Riek R. Somatostatin receptor 1 selective analogues: 4. Three-dimensional consensus structure by NMR. *J. Med. Chem* 2005;48:523–533. [PubMed: 15658866]

**Figure 1.**

Survey of characteristic NOEs used in CYANA for structure calculation for analogues 1-6. Thin, medium and thick bars represent weak (4.5 to 6 Å), medium (3 to 4.5 Å) and strong (< 3 Å) NOEs observed in the NOESY spectrum. The medium-range connectivities $d_{NN}(i,i+2)$, $d_{aN}(i,i+2)$, and $d_{bN}(i,i+2)$ are shown by lines starting and ending at the positions of the residues related by the NOE. Residues designated with X and X' correspond to the amino acid Aph (CONH₂) and Aph(CONHOCH₃), respectively.

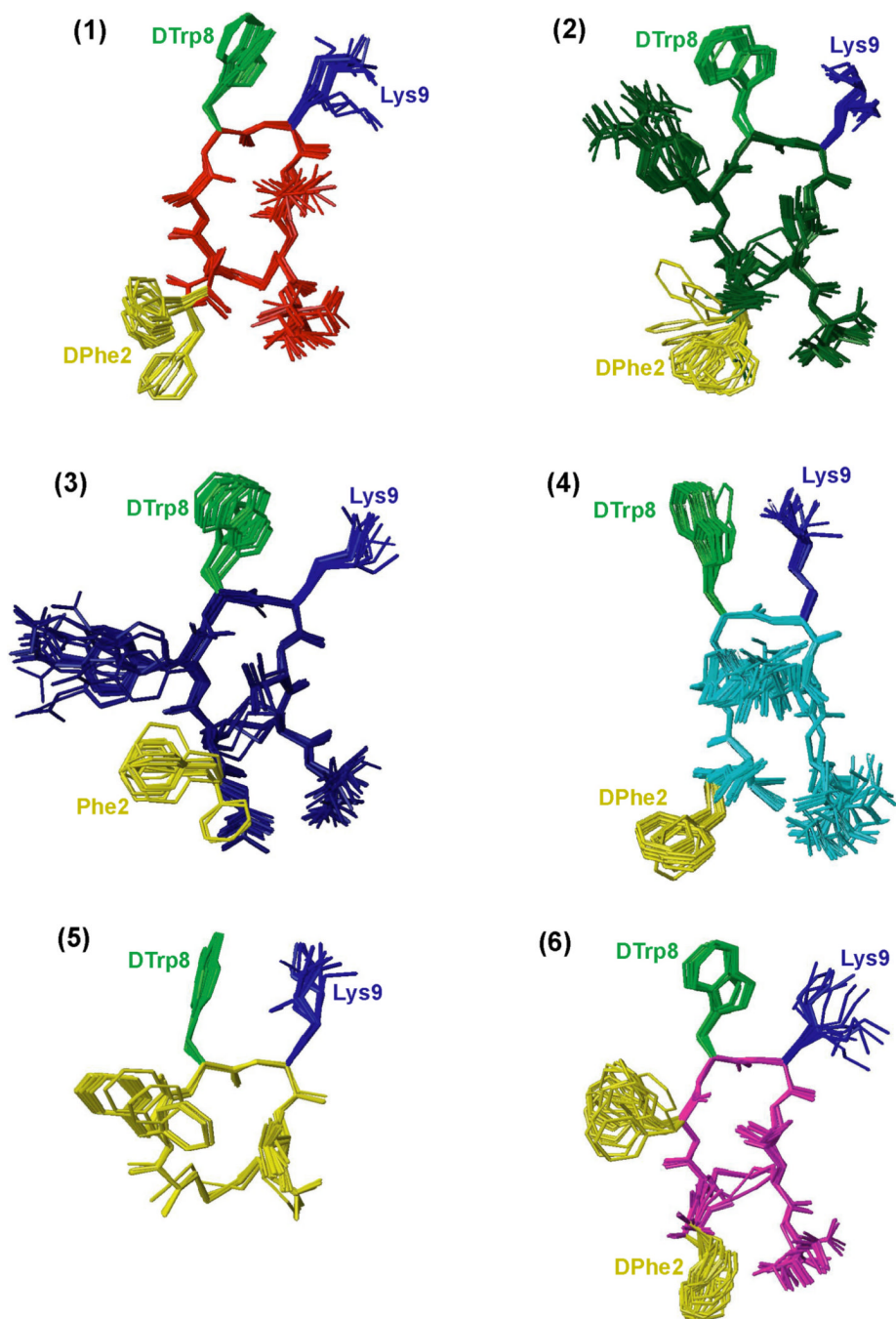


Figure 2. NMR structures of analogues **1–6**. For each analogue, twenty energy-minimized conformers with the lowest target function are used to represent the 3D NMR structure. The bundle is obtained by overlapping the C α atoms of the residues 2–9. The backbone and the side chains are displayed including the disulfide bridge. The following color code is used: red **(1)** H-DPhe-c[Cys-Ala-DTrp-Lys-Thr-Cys]-Thr-NH₂, dark green **(2)** H₂NCO-DPhe-c[Cys-Aph(CONH₂)-DTrp-Lys-Thr-Cys]-Thr-NH₂, navy blue **(3)** H₂NCO-Phe-c[Cys-Aph(CONH₂)-DTrp-Lys-Thr-Cys]-Thr-NH₂, cyan **(4)** H₂NCO-DPhe-c[Cys-Aph(CONHOCH₃)-DTrp-Lys-Thr-Cys]-Thr-NH₂, yellow **(5)** H-c[Cys-Phe-DTrp-Lys-Thr-Cys]-OH, magenta **(6)** H-DPhe-c[Cys-Phe-DTrp-Lys-Thr-Cys]-Thr-NH₂. The side chains that are involved in sst₂-binding are

highlighted; these are DTrp at position 8 in light green, Lys at position 9 in blue and DPhe or Phe at position 2 in yellow.

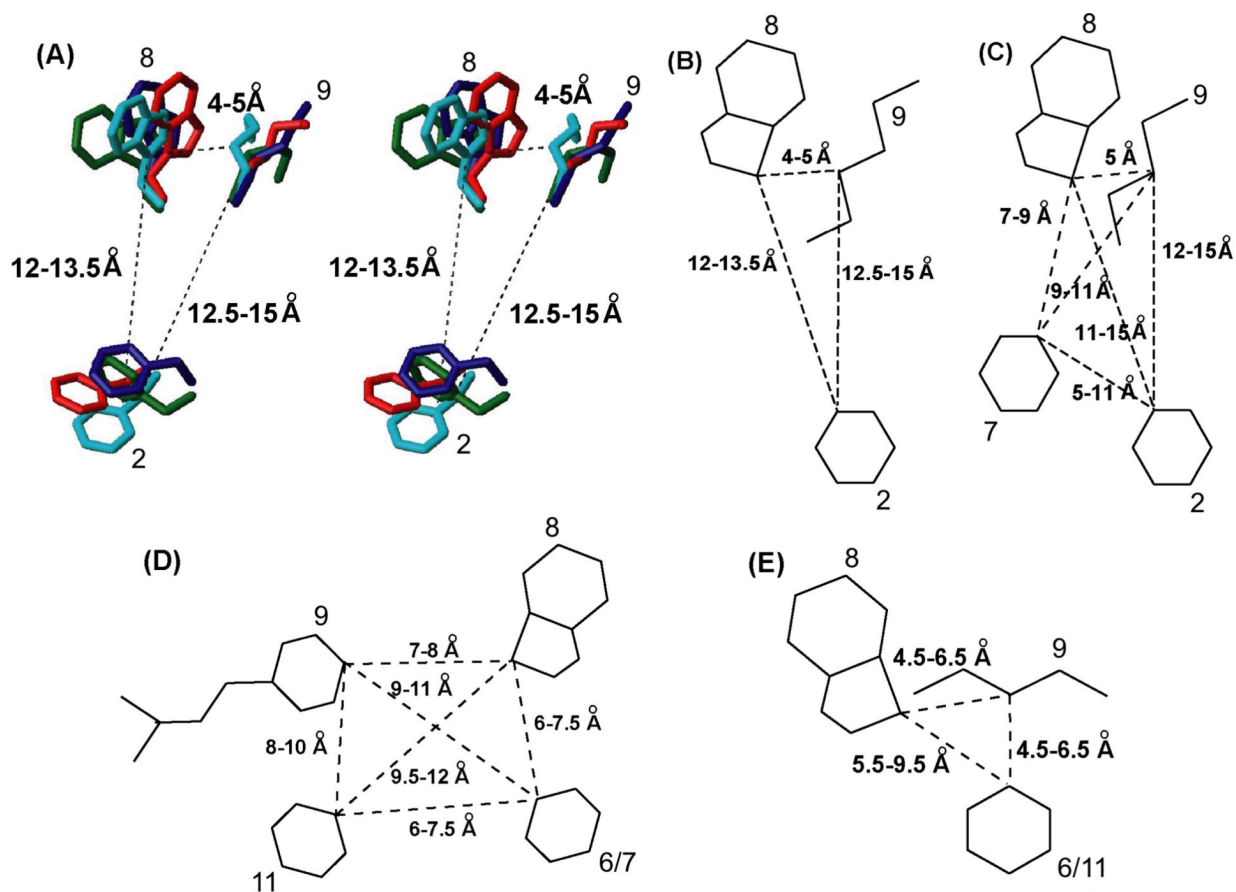


Figure 3.

Consensus structural motif of $ss\tau_2$ -selective SRIF analogues. (A) Stereo view of the consensus structural motif for the $ss\tau_2$ -selective analogues **1** (red), **2** (green), **3** (navy blue) and **4** (cyan). Only the side chains of the residues DPhe², DTrp⁸ and Lys⁹ for **1**, **2**, **3** and **4** are shown. The distances between the C γ atoms of DTrp⁸, Lys⁹ and DPhe² are displayed. For each analogue, the conformer with the lowest target function is displayed. (B) Schematic drawing of the pharmacophore for the $ss\tau_2$ -selective SRIF analogues. (C) Schematic drawing of the pharmacophore for the $ss\tau_{2/3/5}$ -selective SRIF analogues.¹⁶ (D) Schematic drawing of the pharmacophore for the $ss\tau_1$ -selective SRIF analogues.⁶² (E) Schematic drawing of the pharmacophore for the $ss\tau_4$ -selective SRIF analogues.²⁰ In all of the pharmacophores, the distance between the C γ atoms of the respective residues is displayed.

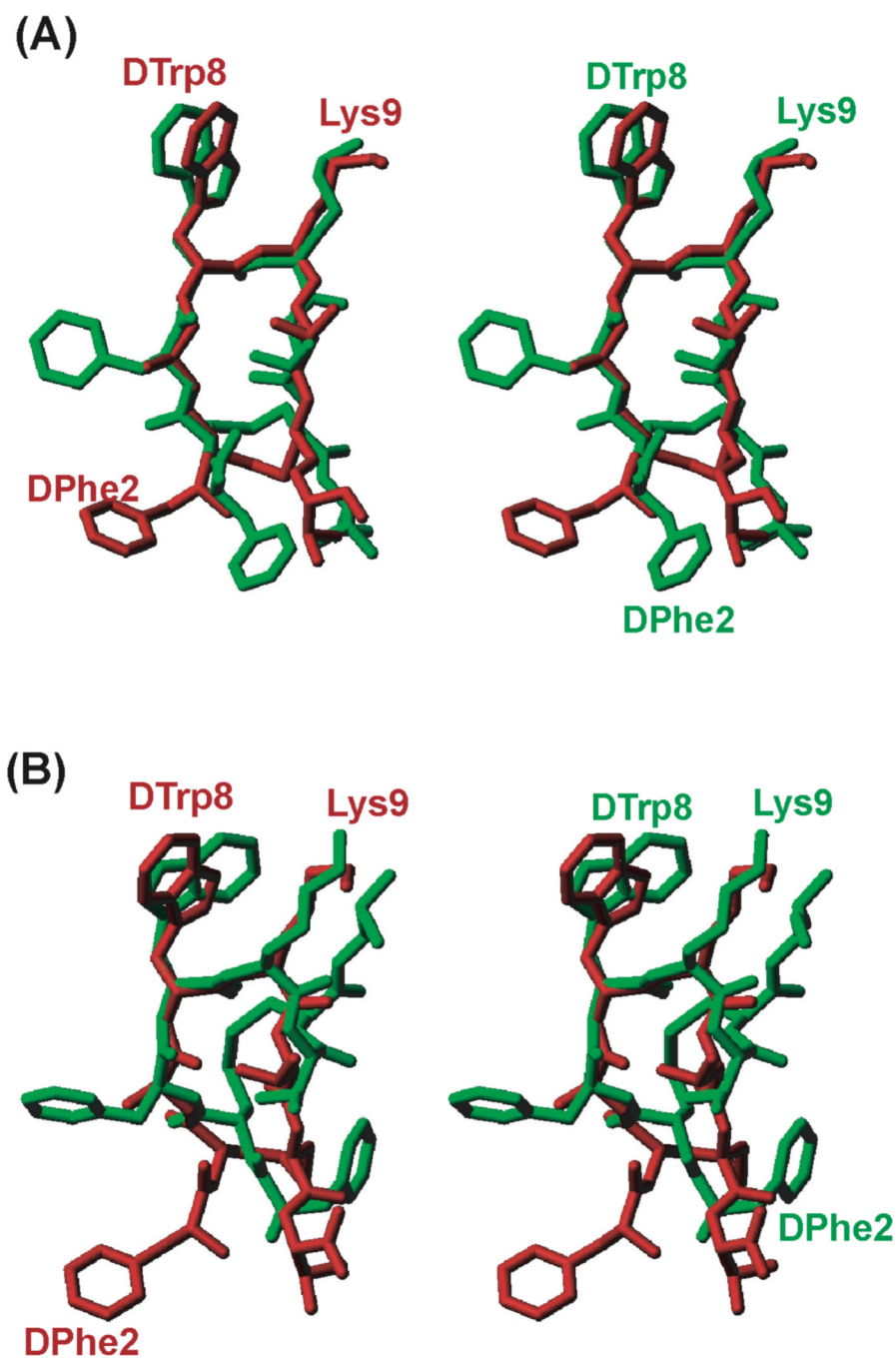


Figure 4. Comparison of the 3D structure of sst₂-selective (analogue **1**) and sst_{2/3/5}-selective (octreotide and analogue **6**) SRIF analogues. Stereo view of the superposition of the 3D structure of the sst₂-selective analogue **1** (red) with the 3D structure of the sst_{2/3/5}-selective octreotide (green) **16** (A) in β -turn conformation and (B) in helical conformation. It must be noted that DPhe² labeled, in both of the analogues is important for selective binding, but differs in its spatial orientation relative to the DTrp⁸-Lys⁹ pair.

Table 1
Physico-chemical properties and sst₁₋₅ binding affinities (IC₅₀s, nM) of analogues studied by NMR.

ID #	Compound	Purity (%)		MS ^c			IC ₅₀ nM ^d				
		HPLC ^d	CZE ^b	M (mono) calc.	MH ⁺ (mono) obs.	ss1 ₁	ss1 ₂	ss1 ₃	ss1 ₄	ss1 ₅	
1	H-DPhe-c[Cys-Ala-DTrp-Lys-Thr-Cys]-Thr-NH ₂	99	99	955.40	956.38	>1K (3)	8.6;4.5;3.6	772;~1472;543	>1K (3)	158;807;226	
2	H ₂ N-CO-DPhe-c[Cys-Aph (CONH ₂)-DTrp-Lys-Thr-Cys]-Thr-NH ₂	98	97	1132.45	1133.17	>1K (3)	6.4;9;6.2	210;725;394	>1K; 905;494	400;77;100	
3	H ₂ N-CO-Phe-c[Cys-Aph (CONH ₂)-DTrp-Lys-Thr-Cys]-Thr-NH ₂	98	99	1132.46	1133.44	>1K (2)	7.5;20	942;1094	957;872	109;260	
4	H ₂ N-CO-DPhe-c[Cys-Aph (CONHOCH ₃)-DTrp-Lys-Thr-Cys]-Thr-NH ₂	99	99	1119.46	1120.42	>1K (2)	3.1;4.4	>1K;958	>1K (2)	808;539	
5	H-c[Cys-Phe-DTrp-Lys-Thr-Cys]-OH	97	98	784.30	785.27	>1K	378	>1K	>1K	>1K	
6	H-DPhe-c[Cys-Phe-DTrp-Lys-Thr-Cys]-Thr-NH ₂	95	99	1031.43	1032.00	>1K	2.7;2.2	80;38	>10K	2.7;3.9	

^aPercent purity determined by HPLC (Hewlett-Packard Series II 1090 Liquid Chromatograph) using buffer system: A = TEAP (pH 2.5) and B = 60% CH₃CN/40% A with a gradient slope of 1% B/min, at flow rate of 0.2 mL/min on a Vydac C₁₈ column (0.21 × 15 cm, 5-μm particle size, 300 Å pore size). Detection at 214 nm.

^bCapillary zone electrophoresis (CZE) was done using a Beckman P/ACE System 2050 controlled by an IBM Personal System/2 Model 50Z and using a ChromJet integrator. Field strength of 15 kV at 30 °C, mobile phase: 100 mM sodium phosphate (85:15, H₂O:CH₃CN) pH 2.50, on a Supelco P175 capillary (363 μm OD x 75 μm ID X 50 cm length). Detection at 214 nm.

^cMass spectra (MALDI-MS) were measured on an ABI-PerSeptive DE-STR instrument. The instrument employs a nitrogen laser (337 nm) at a repetition rate of 20 Hz. The applied accelerating voltage was 20 kV. Spectra were recorded in delayed extraction mode (300 ns delay). All spectra were recorded in the positive reflector mode. Spectra were sums of 100 laser shots. Matrix: α-cyano-4-hydroxycinnamic acid was prepared as saturated solutions in 0.3% trifluoroacetic acid and 50% acetonitrile. The observed monoisotopic (M + H)⁺ values of each peptide corresponded with the calculated (M + H)⁺ values.

^dThe IC₅₀ values (nM) were derived from competitive radioligand displacement assays reflect the affinities of the analogues for the cloned somatostatin receptors using the non-selective [¹²⁵I]-[Leu⁸,DTrp²²,Tyr²⁵]SRIF-28, as the radioligand.

Table 2

Proton chemical shifts of analogues 1–6*

Residue	¹ H	Analogues					
		1	2	3	4	5	6
H ₂ N-CO			5.42	5.66	7.59		
	NH	7.99	6.33	6.42	8.01		
	αH	4.20	4.55	4.53	4.19		
	βH	3.22,2.96	3.08,2.72	3.00,2.80	3.25,2.95		4.15 3.24,2.95
dPhe/Phe ²	H2,6	7.38	7.28	7.14	7.38		7.38
	H3,5	7.29	7.23	7.21	7.30		7.29
	NH	9.22	8.72	8.59	9.23		9.22
	αH	5.27	5.22	5.16	5.27		5.28
Cys ³	βH	2.76,2.82	2.77,2.77	2.81,2.81	2.82,2.82		2.81,2.81
		Ala	Aph(CONH ₂)	Aph(CONH ₂)	Aph(CONHOCH ₃)	Phe	Phe
	NH	8.44	8.49	8.45	8.52	8.36	8.55
	αH	4.47	4.58	4.60	4.65	4.67	4.66
Aph/Ala ⁷	βCH ₃	1.17					
	βH		2.77,2.77	2.81,2.81	2.79,2.79	2.81,2.81	2.84,2.84
	H2,6		6.96	6.99	7.03	7.03	7.08
	H3,5		7.22	7.28	7.44	7.16	7.17
	HT		8.46	8.54	8.84		
	NH ₂		5.86	5.92	9.55		
	CH ₃				3.62		
	NH	8.92	8.82	8.80	8.81	8.74	8.77
	αH	4.30	4.20	4.19	4.19	4.58	4.19
	βH	3.07,2.99	2.98,2.73	2.98,2.72	2.98,2.73	3.14,2.86	2.96,2.71
dTrp ⁸	HDI	7.19	6.93	6.91	6.97	6.99	6.95
	HE1	10.87	10.76	10.77	10.74	10.80	10.81
	HZ2	7.32	7.29	7.30	7.29	7.32	7.32
	HH2	7.06	7.04	7.06	7.04	7.08	7.06
	HZ3	6.99	6.98	7.00	6.99	7.00	6.99
	HE3	7.54	7.42	7.41	7.41	7.47	7.43
	NH	8.43	8.36	8.39	8.40	8.50	8.46
	αH	3.99	4.01	4.00	3.97	3.89	3.99
	βH	1.70,1.25	1.72,1.27	1.73,1.29	1.70,1.26	1.69,1.37	1.72,1.30
	γH	0.72,0.72	0.77,0.74	0.80,0.76	0.76,0.72	0.86,0.86	0.79,0.79
Lys ⁹	δH	1.29,1.29	1.30,1.30	1.32,1.32	1.32,1.32	1.35,1.35	1.35,1.35
	εH	2.55,2.55	2.56,2.56	2.58,2.58	2.55,2.55	2.60,2.60	2.57,2.57
	εNH	7.60	7.56	7.62	7.58	7.63	7.62
Residue							
Thr ¹⁰							
Cys ¹⁴							

Residue	¹ H	Analogues					
		1	2	3	4	5	6
Thr ¹⁵	βH	2.86,2.86	2.85,2.85	2.84,2.84	2.86,2.86	3.14,2.86	2.86,2.86
	NH	8.06	8.17	8.13	8.05		8.07
	αH	4.22	4.21	4.23	4.23		4.21
	βH	4.02	4.06	3.93	4.03		4.03
	γH	1.05	1.07	0.99	1.07		1.06
NH ₂		5.15	5.13	5.07	5.15		
		7.53,7.36	7.42,7.26	7.43,7.35	7.53,7.36		7.35,7.52

* The chemical shifts were measured at 298K in DMSO in ppm with the internal reference of the DMSO signal at 2.49 ppm.

Table 3

Characterization of the NMR structures of analogues 1–6*

ID#	NOE distance restraints	Angle restraints ^{****}	CYANA Target ^{***} function	Backbone RMSD (Å)	Overall RMSD (Å)	CFF91 energies (Kcal/mol)		Residual restraint violations on Distances		Dihedral Angles		
						Total energy	Van der Waals	Electrostatic	No. ≥ 0.1 Å	Max (Å)	No. ≥ 1.5 deg	Max (deg)
1	131	24	0.005	0.52 ± 0.09	1.03 ± 0.20	178 ± 7	89 ± 4	89 ± 7	0.7 ± 0.1	0.11 ± 0.01	0 ± 0	0 ± 0
2	135	17	0.001	0.44 ± 0.24	0.96 ± 0.30	211 ± 10	118 ± 5	93 ± 8	0.2 ± 0.1	0.05 ± 0.01	0 ± 0	0 ± 0
3	130	25	0.003	0.47 ± 0.28	1.07 ± 0.45	204 ± 14	124 ± 11	81 ± 7	0.3 ± 0.1	0.07 ± 0.03	0 ± 0	0 ± 0
4	130	19	0.008	0.73 ± 0.25	1.21 ± 0.31	188 ± 11	116 ± 7	72 ± 6	0.5 ± 0.1	0.10 ± 0.02	0 ± 0	0 ± 0
5	80	14	0.0002	0.08 ± 0.09	0.62 ± 0.19	158 ± 10	86 ± 7	73 ± 13	0.1 ± 0.0	0.03 ± 0.00	0 ± 0	0 ± 0
6	115	24	0.002	0.56 ± 0.14	1.06 ± 0.28	210 ± 14	121 ± 10	89 ± 8	0.4 ± 0.1	0.11 ± 0.02	0 ± 0	0 ± 0

*The bundle of 20 conformers with the lowest residual target function was used to represent the NMR structures of each analogue.

The target function is zero only if all the experimental distance and torsion angle constraints are fulfilled and all non-bonded atom pairs satisfy a check for the absence of steric overlap. The target function is proportional to the sum of the square of the difference between calculated distance and isolated constraint or van der Waals restraints and similarly isolated angular restraints are included in the target function. For the exact definition see reference.³²*Meaningful NOE distance restraints may include intra-residual and sequential NOEs.³²

Table 4Torsion angles ϕ , ψ and χ_1 (in degrees) of the bundle of 20 energy minimized conformers.

Analogue	Angle	DPhe ²	Cys ³	Ala ⁷	DTrp ⁸	Lys ⁹	Thr ¹⁰	Cys ¹⁴	Thr ¹⁵
1	ϕ	-	-33 ± 60	-156 ± 13	72 ± 3	-91 ± 0	-140 ± 4	-156 ± 16	-11 ± 46
	ψ	67 ± 17	87 ± 6	132 ± 3	-146 ± 2	26 ± 1	-149 ± 23	87 ± 8	121 ± 56
	χ_1	108 ± 6	132 ± 3	170 ± 95	-151 ± 3	-128 ± 2	-22 ± 86	176 ± 3	173 ± 54
2	ϕ	121 ± 45	-84 ± 35	Aph(CONH ₂) ⁷	97 ± 14	-103 ± 7	-74 ± 5	87 ± 2	-19 ± 37
	ψ	172 ± 9	117 ± 16	-178 ± 19	-113 ± 14	2 ± 6	-137 ± 8	81 ± 8	110 ± 76
	χ_1	115 ± 32	-121 ± 40	-175 ± 14	150 ± 6	-83 ± 7	-43 ± 7	-143 ± 24	-163 ± 58
3	ϕ	Phe ²		Aph(CONH ₂) ⁷					
	ψ	-149 ± 9	174 ± 38	179 ± 22	95 ± 22	-103 ± 12	-63 ± 5	83 ± 28	-109 ± 59
	χ_1	-145 ± 51	110 ± 11	98 ± 20	-108 ± 7	-8 ± 1	-140 ± 5	78 ± 8	48 ± 87
4	ϕ	-132 ± 30	-144 ± 24	-126 ± 18	-171 ± 6	-105 ± 1	-39 ± 2	-110 ± 34	-129 ± 76
	ψ	DPhe ²		Aph(CONHOCH ₃) ⁷					
	χ_1	175 ± 6	43 ± 2	-111 ± 8	44 ± 5	-141 ± 4	-143 ± 10	167 ± 71	-83 ± 83
5	ψ	41 ± 4	53 ± 5	59 ± 5	-104 ± 3	45 ± 8	165 ± 52	78 ± 14	105 ± 78
	χ_1	98 ± 6	-76 ± 34	-177 ± 5	160 ± 5	-45 ± 8	-52 ± 7	-155 ± 13	118 ± 49
	ϕ			Phe ⁷					
6	ψ			-154 ± 8	156 ± 3	-93 ± 3	-93 ± 3	-54 ± 5	
	χ_1			23 ± 6	-128 ± 3	12 ± 0	2 ± 4	-	
	ϕ			160 ± 38	166 ± 1	-116 ± 0	-62 ± 8	-156 ± 4	
6	ϕ			Phe ⁷					
	ψ	-	-71 ± 28	-173 ± 11	102 ± 2	-93 ± 3	-104 ± 5	-168 ± 5	-89 ± 64
	χ_1	-160 ± 0	-153 ± 66	98 ± 6	-121 ± 0	1 ± 3	45 ± 5	81 ± 3	98 ± 70
		32 ± 0	-117 ± 5	-150 ± 29	-168 ± 1	-126 ± 4	140 ± 8	-148 ± 12	175 ± 4